Impact of environmental factors on mosquito dispersal in the prospect of Sterile Insect Technique control.

Claire Dufourd[a], Yves Dumont[b*]
[a] Department of Mathematics and Applied Mathematics,
University of Pretoria, Pretoria 0002, South Africa
[b]CIRAD, Umr AMAP, TA-A51/PS2,
Boulevard de la Lironde, 34398 Montpellier Cedex 5, France

Abstract

The aim of this paper is to develop a mathematical model to simulate mosquito dispersal and its control taking into account environmental parameters, like wind, temperature, or landscape elements. We particularly focus on *Aedes albopictus* mosquito which is now recognized as a major vector of human arboviruses, like chikungunya, dengue, or yellow fever. One way to prevent those epidemics is to control the vector population. Biological control tools, like the Sterile Insect Technique (SIT), are of great interest as an alternative to chemical control tools which are very detrimental to environment. The success of SIT is based on a good knowledge of the biology of the insect, but also on an accurate modeling of the insect's distribution. We consider a compartmental approach and derive temporal and spatio-temporal models, using Advection-Diffusion-Reaction equations to model mosquito dispersal. Periodic releases of sterilized males are modeled with an impulse differential equation. Finally, using the splitting operator approach, and well-suited numerical methods for each operator, we provide numerical simulations for mosquito spreading, and test different vector control scenarios. We show that environmental parameters, like vegetation, can have a strong influence on mosquito distribution and in the efficiency of vector control tools, like SIT.

keyword Advection diffusion reaction equation, impulse differential equation, mosquito dispersal, sterile insect technique, operator splitting, nonstan-

*Corresponding author: yves.dumont@cirad.fr

dard finite difference method, numerical algorithm. **AMSC**[2010]: 35M, 35Q92, 34B37, 65M06, 65L99

1 Introduction

Since the pioneering work of Sir R. Ross, who showed that the female *Anopheles* mosquito was responsible for malaria transmission [45, 46], our understanding on mosquito biology and ecology has increased. It is now admitted that mosquitoes are responsible for many vector-borne diseases throughout the world, for example chikungunya, dengue, yellow fever, and West Nile virus. Ross was the first to propose vector control as a strategy to reduce the epidemiological risk [47]. Thus, vector control is now commonly used in many places using mechanical, chemical or biological control tools. Even if entomologists have accumulated knowledge and numerous field data, there is a lack in the use of modeling to raise new questions or test biological hypotheses. Indeed, modeling and numerical simulations can provide interesting tools for experts to provide simulations in order to validate or improve vector control strategies with a minimal number of field experiments that can be very difficult to conduct and expensive. This work is the continuation of previous works done on the temporal modeling of chikungunya in Réunion Island [20, 19] and patch modeling [9], the latter being an intermediate approach, between temporal and spatio-temporal models.

In this paper, we intend to develop a model for mosquito dispersal, with a particular emphasize on a specific mosquito species, *Aedes albopictus*, commonly called the "Asian tiger". It is responsible for carrying many diseases, particularly in Africa, in Asia, and in Indian Ocean. This mosquito has spread around the world because of its high biological and ecological plasticity [8, 42]. It has been able to adapt rapidly to a large range of habitats and environmental conditions: from forest environments to urban and suburban environments. Thus, *Ae. albopictus* is also present in European countries, like France, Italy and Spain. Experiments have shown that *Ae. albopictus* is able to complete its life cycle even with mean temperature of $10°C$. Eggs are able to enter dormancy when the temperature becomes too cold and, even, to survive drought during several weeks [42]. *Ae. albopictus* has long been considered as a secondary vector of human pathogens [28] because of its opportunistic feeding behavior: it bites preferentially mammals but can also feed on reptiles, birds and amphibians. Its status has been revisited after the epidemics of chikungunya in Réunion Island in 2006 [17], and in Central Africa [43]. It can also transmit dengue and yellow fever.

In Réunion Island, the control of *Ae. albopictus* started during the dengue epidemics of 2004 with chemical products, like adulticide and larvicide, and mechanical control [19]. Although these tools are useful, they cannot be for long term use, for several reasons. First, Réunion Island is a biodiversity hotspot, vulnerable to prevalent chemical use. Second, mosquitoes can develop resistance to insecticides. And finally, only 10% of the island can be treated, due to its landscape (mountains and gullies). Therefore, it is necessary to consider new sustainable alternatives or additional tools, like the Sterile Insect Technique (SIT). SIT consists in releasing sterilized male mosquitoes that will mate with wild females which won't be able to deposit hatching eggs [32] (see also [6, 1, 23] for extended references about SIT), driving slowly the wild population to decline. Thus, the release of sufficiently many sterile males over a sufficiently long period of time can lead to local reduction or elimination of the wild population. The success of SIT is based on a good knowledge of the biology and the behavior of the vector, but also on an accurate modeling of its dispersal, to optimize the impact of sterile males. Indeed, modeling is helpful not only to formalize knowledge but also to improve release strategies before doing real, long, difficult and expensive experiments. Most of the published models on mosquito population dynamics and SIT are temporal models or/and take only into account one dimensional spatial component (see for instance [38, 37]).

In [18], the model has been presented briefly. Here we enter in more details in the modeling and illustrate the discussions with several simulations. In section 2, we recall biological and ecological facts on *Ae. albopictus* in order to understand our choices in the modeling. In section 3, we first present a compartmental temporal model with and without pulsed SIT, with some theoretical results (existence and uniqueness of a solution, existence of equilibria, local and global stability), and build a dynamically consistant nonstandard finite difference scheme to preserve most of the properties of the continuous system. Afterwards, we extend the temporal model to a spatio-temporal model, which leads to a system of coupled nonlinear advection-reaction-diffusion equations. Then, using the operator splitting technique and appropriate numerical methods for each operator, we build a numerical algorithm to solve the nonlinear system. Finally, in section 4, we provide some numerical simulations: we show that small and frequent releases of sterile males are more efficient than bigger and less frequent releases [23]. We also show the influence of environmental factors, like the landscape, the temperature, or the wind, on the distribution of female mosquitoes and, thus, on SIT control strategies.

2 The biology and behavior of *Aedes albopictus*

In order to develop accurate models, we briefly recall some biological knowledge about *Ae. albopictus* in Réunion Island [16]. There are two main stages in the development of mosquitoes: an aquatic and an adult stage. The aquatic stage gathers eggs, larvae and pupae. The adult stage can be divided in several compartments: immature females, feeding females, resting females, breeding females (or more precisely "egg laying females") and males. In a previous paper [21], we have built a spatio-temporal model with only two compartments for the female mosquitoes: feeding females and breeding females. This was sufficient enough given that we were studying the impact of classical vector control (mechanical and chemical). Here, in order to model efficiently SIT control, we need to consider more compartments.

Since we assume no sex differences in the aquatic stage, mosquitoes, after emergence, are distributed between the immature female compartment and the male compartment. Following [16], we consider that the number of emerging females and emerging males is equal; therefore the sex ratio of emerging adults, r, is set to $\frac{1}{2}$. We assume that a female mates only once with a male in her lifetime. After mating with males, we assume that immature females start their gonotrophic cycles [16] by entering the feeding female compartment. The gonotrophic cycle defined by Clements [12] starts with a blood meal and ends with the first laid egg. Then, after blood meals, they get into the resting compartment, allowing egg maturation. Afterwards, the females pass into the breeding compartment seeking for a breeding site to deposit eggs. Once eggs deposit is done, females start a new gonotrophic cycle. The eggs laid by the breeding females supply the aquatic stage. We consider only one compartment for the males. For the females, it is necessary to take into account the three sub-compartments since their behavior is very different.

In order to simulate SIT control, we add a sterile male compartment. Sterile males come from (periodic pulsed) releases in specific places. The transition rate between the immature females and the feeding females is conditioned by the proportion of non-sterile and competitive males to the whole male population that are near immature females. The biological cycle of *Ae. albopictus* as described above is represented in Fig. 1, page 5.

In Fig. 1, parameters M_A, M_Y, M_f, M_m and M_{ms} are respectively the mortality rates for the aquatic stage, the immature females, the mature females, the wild males and the sterilized males. M_Y and M_f will be assumed to be equal. η_A is the emergence rate, β_Y is the rate at which immature females become blood-feeding females. $1/(M_Y + \beta_Y)$ represents the average

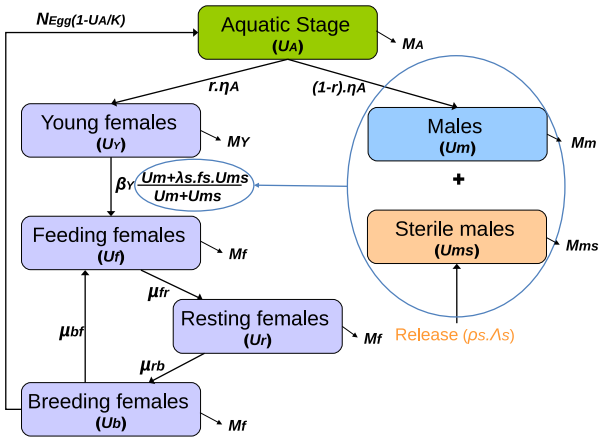

Figure 1: Biological cycle of *Aedes albopictus* with releases of sterile males

time spent by a female mosquito in the immature stage, i.e. between emergence and the first blood meal. It has been shown that *Aedes* males are sexually very active: one male can mate, on average, 8-9 immature females per day [11]. Thus, whatever the wild male density, an emerging female will either mate rapidly and then enters the blood feeding compartment or die. Therefore, due to the "exceptional" mating capacity of wild males, it is not necessary to consider an encounter probability between wild males and young females in the wild population model. μ_{fr} is the rate at which blood-feeding females become resting females, μ_{rb} is the rate at which resting females become breeding females, and μ_{bf} is the rate at which breeding females become blood-feeding females, N_{Egg} is the average number of eggs laid per female, K is the carrying capacity of a breeding site, Λ_s is the number of sterile males released with a rate of $(1 - \lambda_s)$ effective sterilisation. The efficiency of SIT depends on the quality of the release, ρ_s, and the sexual competitivity between sterile males and wild males, f_s. If the release is far from the females, then sterile males will have lower chance to mate females, so, $\rho_s\Lambda_s$ may represent the release of sterile males that would actually play a role in SIT. Following [1, 23], we assume that the probability for an immature female to become a feeding female depends on the ratio $(u_M + \lambda_s f_s u_{Ms})/(u_M + u_{Ms})$, when sterile males are released. Note that ρ_s is only relevant in the temporal model, as it provides some kind of spatial information on the releases. Without any relevant informations about the spreading ability of sterile males,

we assume that they have the similar ability than wild ones. Finally, according to Delatte et al. [16], some biological parameters of *Ae. albopictus* are temperature-dependant, whereas others not.

2.1 Constant and Temperature-varying parameters

In Table 1 we summarize parameters that are not importantly impacted when the temperature varies from $15°C$ to $35°C$. These include the proportion of females to the whole population, r, the average number of eggs laid per day, N_{Egg}, the transition rates β_Y, μ_{bf} and μ_{fr}.

Parameter	Unit	Value	Source
r	-	0.5	[16]
N_{Egg}	$\text{female}^{-1}\text{day}^{-1}$	≈ 60	Table 6 in [16]
μ_{bf}	day^{-1}	$\approx 1/3$	Table 6 in [16]
μ_{fr}	day^{-1}	≈ 1	*
$\beta_Y + M_Y$	day^{-1}	$\approx 1/5$	Table 4 in [16]

Table 1: Values of constant parameters. *We assume that females stay in mean 1 day in the feeding compartment.

Param	Unit	$10°C$	$15°C$	$20°C$	$25°C$	$30°C$	$35°C$	$40°C$
M_A	day^{-1}	1	0.959	0.4815	0.6246	0.6530	0.9975	1
η_A	day^{-1}	0	0.0236	0.0578	0.0671	0.0645	0.0515	0
d_G	day	-	-	8.1	4.5	3.5	4.4	-
μ_{rb}	day^{-1}	-	-	0.14	0.286	0.4	0.294	-
M_f	day^{-1}	-	0.0259	0.0322	0.0322	0.029	0.0504	-
M_m	day^{-1}	-	0.0319	0.0484	0.0512	0.0573	0.0671	-

Table 2: Values of temperature-varying parameters [16]

In Table 2, we present the temperature-varying parameters, according to [16]. The mortality rate of the aquatic stage, M_A, is calculated using the hatching rate and the probability of survival from the first stage of larvae the adult stage [16]. The parameter $1/(M_A + \eta_A)$ is the average time spent in the aquatic stage. d_G being the average duration of a gonotrophic cycle, we have $d_G = \frac{1}{\mu_{fr}} + \frac{1}{\mu_{rb}}$. Since μ_{bf} and μ_{fr} are constant, we deduce the value of μ_{rb} for each temperature: $\mu_{rb} = 1/(d_G - \frac{1}{\mu_{fr}})$ (see Table 2). Since we consider continuous variations of the temperature, we interpolate the parameters given in Table 2, using monotonic cubic spline interpolation [26] (see Fig. 2, page 7).

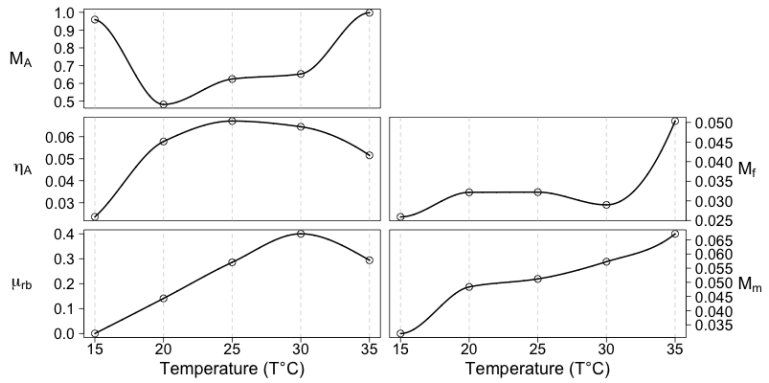

Figure 2: Graphs of the interpolation for temperature-varying parameters, using monotonic cubic spline interpolation [26].

The capacity, K, of the breeding sites varies along the year according to the climate. A rainy period can lead to the creation of new breeding sites, or increase the capacity of the existing ones. On contrary, a dry period can reduce the number of breeding sites, or reduce the capacity of existing ones. However it is very difficult to give an estimate for K on a given area due to the great varability of the breeding sites. For instance, a pound can be a breeding site, and will be there probably during the whole year. Other breeding sites are more or less temporary, like puddles that can be created easily but that can also dry very fast. Breeding sites can be found in many unsuspected places since any object susceptible to retain water (after a rain) could become a breeding site, like tires or plant saucers. In order to take into account the varying global capacity of breeding sites, we assume that the capacity is maximum, $K = K_{max}$, at 27°, which is the mean temperature at the end of the rainy season in Réunion Island. We assume that 15° corresponds to austral winter, when the precipitations are low (dry season), and the capacity is at the lowest, $K = K_{min}$. We assumed that $K_{min} = 0.1 \times K_{max}$. Therefore, we assume that K increases according to a temperature between 15° and 27°. When the temperature is above 27°, we assume that K decreases either due to evaporation and to the fact that too heavy rains can be detrimental to breeding sites. We assume that $K = 0.75 \times K_{max}$ at 35° We obtain a continuous relation between K and the temperature using a linear interpolation.

3 Temporal and spatio-temporal models

In the following section, we present models with constant and temperature varying parameters. We first present the temporal model as it will be related to the reaction operator in the spatio-temporal model. A qualitative study is also necessary to build an appropriate numerical scheme to solve the temporal model, and then the reaction operator in the splitting operator approach.

3.1 Temporal modeling of the wild mosquito population

Following Fig. 1 and using all biological explanations, we derive the following temporal model for the wild mosquito population:

$$\left\{\begin{array}{rcl} \frac{du_A}{dt} &=& N_{Egg}(1-\frac{u_A}{K})u_b - (\eta_A + M_A)u_A, \\ \frac{du_Y}{dt} &=& r\eta_A u_A - (M_Y + \beta_Y)u_Y, \\ \frac{du_f}{dt} &=& \mu_{bf}u_b + \beta_Y u_Y - (M_f + \mu_{fr})u_f, \\ \frac{du_r}{dt} &=& \mu_{fr}u_f - (M_f + \mu_{rb})u_r, \\ \frac{du_b}{dt} &=& \mu_{rb}u_r - (M_f + \mu_{bf})u_b, \\ \frac{du_M}{dt} &=& (1-r)\eta_A u_A - M_m u_M, \end{array}\right. \tag{1}$$

The previous system can be rewritten like $\dot{X} = \mathcal{A}(X)X$, with $X = (u_A, u_Y, u_f, u_r, u_b, u_M)^T$ and $\mathcal{A}(X) =$

$$\begin{pmatrix} -\left(\frac{N_{Egg}}{K}u_b + \eta_A + M_A\right) & 0 & 0 & 0 & N_{Egg} & 0 \\ r\eta_A & -(M_Y+\beta_Y) & 0 & 0 & 0 & 0 \\ 0 & \beta_Y & -(M_f+\mu_{fr}) & 0 & \mu_{bf} & 0 \\ 0 & 0 & \mu_{fr} & -(M_f+\mu_{rb}) & 0 & 0 \\ 0 & 0 & 0 & \mu_{rb} & -(M_f+\mu_{bf}) & 0 \\ (1-r)\eta_A & 0 & 0 & 0 & 0 & -M_m \end{pmatrix}$$

The right-hand side of system (1) is Lipschitz continuous, and thus from classical analysis we deduce that there exists a unique maximal solution. Note also that $\mathcal{A}(X)$ is a Metzler matrix (all components, except the ones in the diagonal, are non-negative [25]), which implies that the solution stays in the positive orthant provided that the initial condition is given in the positive orthant. Moreover, straighforward computations show that the solution is bounded. Thus, Model (1) is said to be biologically well posed.

Remark 1. *The previous existence and uniqueness result holds even if some parameters are time (temperature)-dependent and continuous. In that case, we obtain a nonlinear non-autonomous system* $\dot{x} = F(x,t) = A(t)x + g(x,t)$,

where g stands for the nonlinear term in the aquatic stage. Assuming that all parameters are strictly positive and bounded from above, it is possible to verify that F is continuous and Lipschitz continuous, such that there exists a local solution. Using a comparison principle, we insure that the solution is always positive and bounded.

Remark 2. *If we assume that some parameters are continuous and periodic, system (1) has a positive periodic solution [50].*

Let us now give a brief theoretical and numerical analysis of (1), that will be useful to develop the numerical algorithm for the whole model.

3.1.1 Theoretical analysis

Let us first look for the equilibria of system (1). Setting

$$R_0 = \frac{N_{Egg}\mu_{rb}\mu_{fr}\beta_Y r\eta_A}{(\eta_A + M_A)(M_Y + \beta_Y)\left((M_f + \mu_{fr})(M_f + \mu_{bf})(M_f + \mu_{rb}) - \mu_{bf}\mu_{rb}\mu_{fr}\right)}, \tag{2}$$

after some straighforward computations, we show:

Proposition 1. *There exists a trivial equilibrium for (1),* $TE = (0, 0, 0, 0, 0)^T$. *When* $R_0 > 1$, *there exists another non trivial equilibrium* $E = (u_A^*, u_Y^*, u_f^*, u_r^*, u_b^*, u_M)^T$ *which is biologically realistic:*

$$\left\{\begin{array}{lcl} u_A^* & = & \frac{R_0-1}{R_0}K \\ u_Y^* & = & \frac{r\eta_A}{(\beta_Y+M_Y)}u_A^* = \frac{r\eta_A}{(\beta_Y+M_Y)}\frac{R_0-1}{R_0}K \\ u_f^* & = & \frac{\beta_Y r\eta_A}{(M_Y+\beta_Y)(1-S)}u_A^* = \frac{\beta_Y r\eta_A}{(M_Y+\beta_Y)(1-S)}\frac{R_0-1}{R_0}K \\ u_r^* & = & \frac{\mu_{fr}}{(\mu_{rb}+M_f)}u_f^* = \frac{\mu_{fr}\beta_Y r\eta_A}{(\mu_{rb}+M_f)(M_Y+\beta_Y)(1-S)}\frac{R_0-1}{R_0}K \\ u_b^* & = & \frac{\mu_{rb}}{(\mu_{bf}+M_f)}u_r^* = \frac{\mu_{rb}\mu_{fr}\beta_Y r\eta_A}{(\mu_{bf}+M_f)(\mu_{rb}+M_f)(M_Y+\beta_Y)(1-S)}\frac{R_0-1}{R_0}K \\ u_M^* & = & \frac{(1-r)\eta_A}{M_m}u_A^* = \frac{(1-r)\eta_A}{M_m}\frac{R_0-1}{R_0}K \end{array}\right. \tag{3}$$

where $S = \frac{\mu_{bf}\mu_{rb}\mu_{fr}}{(M_f+\mu_{bf})(M_f+\mu_{rb})(M_f+\mu_{fr})}$.

R_0 is usually called the basic reproductive number. Let us now derive some useful results about the stability/instability of the previous equilibria. Values of R_0 and of the theoretical equilibrium of each compartments evaluated at different temperatures are provided in Table 3.

We establish the following results:

	$15°C$	$20°C$	$25°C$	$30°C$	$35°C$	$40°C$
R_0	0	21.29	28.96	35.42	8.49	0
u_A^*	-	3221	6449	7045	5293	-
u_Y^*	-	401	932	993	545	-
u_f^*	-	277	876	1160	353	-
u_r^*	-	1599	2755	2704	1025	-
u_b^*	-	616	2153	2985	786	-
u_M^*	-	1924	4227	3968	2033	-

Table 3: Basic repoductive number (R_0) and theoretical equilibrium evaluated at $15°C$, $20°C$, $25°C$, $30°C$, $35°C$ and $40°C$, for $K_{max} = 8000$

Proposition 2. *1. The trivial equilibrium TE is locally asymptotically stable (LAS) whenever $R_0 < 1$, and unstable otherwise.*

2. The non trivial equilibrium E exists and is LAS whenever $R_0 > 1$, and unstable otherwise.

Proof. See Appendix A □

Theorem 1. *1. When $R_0 \leq 1$, TE is globally asymptotically stable (GAS) on $\mathbb{R}_+^6$.*

2. When $R_0 > 1$, E is GAS on $\mathbb{R}_+^6 \backslash \{0\}$.

Proof. See Appendix B. □

3.1.2 Wild mosquitoes with SIT control

We extend model (1), by adding a compartment of sterile males, u_{Ms}, with pulsed releases, like in [23], but with a slight modification:

$$\begin{cases} \frac{du_A}{dt} &= N_{Egg}(1-\frac{u_A}{K})u_b - (\eta_A + M_A)u_A, \\ \frac{du_Y}{dt} &= r\eta_A u_A - (M_Y + \beta_Y)u_Y, \\ \frac{du_f}{dt} &= \mu_{bf}u_b + \frac{u_M + \lambda_s f_s u_{Ms}}{u_M + u_{Ms}}\beta_Y u_Y - (M_f + \mu_{fr})u_f, \\ \frac{du_r}{dt} &= \mu_{fr}u_f - (M_f + \mu_{rb})u_r, \\ \frac{du_b}{dt} &= \mu_{rb}u_r - (M_f + \mu_{bf})u_b, \\ \frac{du_M}{dt} &= (1-r)\eta_A u_A - M_m u_M, \\ \frac{du_{Ms}}{dt} &= -M_{ms}u_{Ms}, \\ u_{Ms}(T_{start} + n\tau^+) &= u_{Ms}(T_{start} + n\tau) + \rho_s\Lambda_s, \qquad n = 1, 2, 3, ... \end{cases} \tag{4}$$

The number of young females that become feeding-females compartment is conditioned by the ratio $(u_M + \lambda_s f_s u_{Ms})/(u_M + u_{Ms})$ which gives the proportion of non-sterile males with which young females can mate. In addition to [23], we consider a parameter λ_s that indicates the level of fertility of sterile males. In fact, depending on the radiation dose, the sterile male is not necessarily fully sterilized [5, 7]: only for doses greater or equal to 40 Gy, *Aedes* males become fully sterile, i.e. $\lambda_s = 0$. As far as we know, this is the first time that such an assumption is considered in SIT modeling.

The sterile male compartment is supplied with pulsed releases, with a periodicity of τ days, with T_{start}, the starting date of the releases. Λ_s is the number of sterile males per release. $\rho_s \in [0, 1]$ and represents the quality of a release. A release can have poor or good quality according to the distance at which sterile males are released from young females, or according to various environmental factors, like the weather. When ρ_s is close to 0, the release is not appropriate, whereas an optimal release corresponds to $\rho_s = 1$. Finally, parameter f_s represents the sexual competitivity of sterile males [40]. Thus, $\rho_s\Lambda_s$ may represent the release of "efficient" sterile males.

If we set $F_{em} = u_f + u_b + u_r$, model (4) reduces to the model (31) studied in [23]. Thus, most of the results obtained for the pulsed temporal SIT model (31) are still available here: existence of a unique solution, of a trivial equilibrium and a periodic positive equilibrium that are locally asymptotically stable [23].

3.2 The Numerical scheme: a nonstandard finite difference approach

The qualitative study shows that the solution of (1) has several qualitative properties (nonnegative solution, stable and unstable equilibria according to R_0) that we would like to preserve when constructing a numerical algorithms to obtain reliable numerical approximations of the solution. Let us first recall what is a nonstandard finite difference (NSFD) scheme. Consider the differential system:

$$\dot{y} = f(y), \quad y(0) = y_0, \tag{5}$$

and the numerical scheme of the form

$$y^{n+1} = F(\Delta t; y^n), \tag{6}$$

where F follows the usual consistency conditions for the argument $F(0; y) = y$ and $\frac{F(0)}{\Delta t}(y) = f(y)$. To develop such a scheme we will consider the nonstandard finite difference approach [39, 3]. In recent works, it has been shown that this type of finite difference scheme is able to preserve the positivity, the equilibria, the local or global asymptotic stability (instability) of the different equilibria, as well as bifurcation property [2, 4]. Nonstandard methods have been applied successfully on various problems in epidemiology [4, 20, 19, 23], in ecology [22] and in mechanics [24]. Let us recall the following definition:

Definition 1 ([3]). *A finite difference equation (6) that determines approximate solutions y^n to the solution $y(t)$ of a differential equation (5) is called a nonstandard finite difference (NSFD) scheme if at least one of the following two conditions is met:*

- *The classical denominator Δt of the discrete derivative is replaced by a nonnegative function $\Phi(\Delta t)$ such that $\Phi(\Delta t) = \Delta t + O(\Delta t^2)$ as Δt goes to 0.*
- *Nonlinear terms that occur in the right-hand side $f(y)$ of (5) are approximated in a nonlocal way, i.e., by a suitable function of several points of the mesh.*

Definition 2 ([3]). *A NSFD scheme is called (qualitatively) stable or dynamically consistent with respect to some property P of the differential equation, whenever the discrete equation replicates the property P for every value of Δt.*

Definition 3. *A NSFD scheme is called elementary stable whenever the discrete equation preserves the local stability/instability property of any hyperbolic equilibrium.*

Let us now explain in details how to construct a nonstandard scheme for system (1), which can be rewriten as follows

$$\begin{cases} \dfrac{du}{dt} = \left(-A_0(u) + A_1\right) u, \qquad \forall t > 0, \\ u(0) = u_0 \in \mathbb{R}^n_+ \end{cases} \tag{7}$$

where A_0 is a stable Metzler matrix

$$A_0(u) = \begin{pmatrix} \eta_A + M_A + N_{egg}\frac{u_b}{K} & 0 & 0 & 0 & 0 & 0 \\ -r\eta_A & \beta_Y + M_Y & 0 & 0 & 0 & 0 \\ 0 & -\beta_Y & M_f + \mu_{fr} & 0 & -\mu_{bf} & 0 \\ 0 & 0 & -\mu_{fr} & M_f + \mu_{rb} & 0 & 0 \\ 0 & 0 & 0 & -\mu_{rb} & M_f + \mu_{bf} & 0 \\ -(1-r)\eta_A & 0 & 0 & 0 & 0 & \mu_M \end{pmatrix}$$

and A_1 is the following positive matrix

$$A_1 = \begin{pmatrix} 0 & 0 & 0 & 0 & N_{egg} & 0 \\ 0 & 0 & 0 & 0 & 0 & 0 \\ 0 & 0 & 0 & 0 & 0 & 0 \\ 0 & 0 & 0 & 0 & 0 & 0 \\ 0 & 0 & 0 & 0 & 0 & 0 \\ 0 & 0 & 0 & 0 & 0 & 0 \end{pmatrix}$$

Setting u^n an approximation of u at time $t_n = n\Delta t$, for $n = 1, 2, ...,$ and $\Delta t > 0$ the time-step, a possible non-standard scheme is defined as follows

$$\frac{u^{n+1} - u^n}{\phi\left(\Delta t\right)} = -A_0(u^n)u^{n+1} + A_1 u^n,$$

where ϕ is time-step function such that

$$\phi\left(\Delta t\right) = \frac{e^{p\Delta t} - 1}{p},$$

where $p = \max(\eta_A + M_A, M_Y + \beta_Y, M_f + \mu_{fr}, M_f + \mu_{bf}, M_f + \mu_{rb}, M_m)$. Note that the nonlinear term $-N_{egg}\frac{u_b}{K}u_A$ has been treated in a non-local way: one term is explicit, u_b^n, while the other term, u_A^{n+1}, is implicit. Altogether, we have

$$\left(Id + \phi\left(\Delta t\right) A_0(u^n)\right) u^{n+1} = (Id + \phi(\Delta t)A_1)u^n, \tag{8}$$

such that $Id + \phi(\Delta t) A_0(u^n)$ is an M-matrix for all $\Delta t > 0$, which implies that $(Id + \phi(\Delta t) A_0(u^n))^{-1}$ is a positive matrix. Thus our NSFD scheme (8) is positively invariant if $u^0 > 0$. Moreover, it is straighforward to verify that TE and E are fixed points of (8) too. Finally following the proof of Theorem 2, page 402, in [22], our scheme is elementary stable too. Finally NSFD scheme (8) is qualitatively stable.

If we consider system (4), with sterile males, then we have the following new equations to handle:

$$\left\{\begin{array}{lcl} \frac{du_f}{dt} & = & \mu_{bf} u_b + \frac{u_M + \lambda_s f_s u_{Ms}}{u_M + u_{Ms}} \beta_Y u_Y - (M_f + \mu_{fr}) u_f, \\ \frac{du_{Ms}}{dt} & = & -M_{ms} u_{Ms}, \\ u_{Ms}(T_{start} + k\tau^+) & = & u_{Ms}(T_{start} + k\tau) + \rho_s \Lambda_s, \qquad k = 1, 2, 3, ... \end{array}\right.$$

Then following the construction rules, the NSFD schemes related to the sterile males and the mature females are

$$\left\{\begin{array}{l} \frac{u_{Ms}^{k+1} - u_{Ms}^k}{\phi(\Delta t)} = -M_{ms} u_{Ms}^{k+1}, \quad n \leq k < n + j \\ \left(u_{Ms}^{n+j}\right)^+ = u_{Ms}^{n+j} + \rho_s \Lambda_s \end{array}\right. \tag{9}$$

and

$$\frac{u_f^{n+1} - u_f^n}{\phi(\Delta t)} = \mu_{bf} u_b^{n+1} + \frac{u_M^n + \lambda_s f_s u_{Ms}^n}{u_M^n + u_{Ms}^n} \beta_Y u_Y^{n+1} - (M_f + \mu_{fr}) u_f^{n+1},$$

With these choices, it is obvious that the previous discrete equations are positively invariant if the initial conditions are positive. Between t_n and t_{n+j}, the scheme $(9)_1$ is exact, which means that it gives the exact solution whatever the size of the time-step. Finally, including $(9)_2$, we obtain the exact scheme related to the sterile males equation. Altogether, the NSFD scheme related to system (4) is qualitatively stable too.

3.3 The spatio-temporal model

We now extend model (1) (and model (4)) taking into account the spatial component in the modeling. We first give some additional assumptions related to mosquito displacements and behavior.

When mosquitoes are not submitted to stimuli, it is possible to assume that they move randomly in any direction [15]. This leads to a diffusion equation which can be extended to take into account the landscape heterogeneity or correlated random walk. Therefore, we have to incorporate

advection terms or drift terms when mosquitoes, stimulated by attractants, move preferably in certain directions.

For simplicity, we consider a generic equation to model the spread of a mosquito population. It is now well recognized that the environment heterogeneity can have an important effect [36]: this is taken into account in the model by assuming spatial and temporal variations in the parameters. So, let u represent the density of insects, then, one possible model is given by the following general advection-diffusion-reaction equation:

$$\begin{cases} \dfrac{\partial u}{\partial t} = \nabla\left(D\nabla u\right) - \nabla\left(\left(\nabla C + V\right)u\right) + g, & x \in \Omega \text{ and } t > 0, \\ u\left(x,0\right) = u_0\left(x\right) \geq 0, & x \in \Omega \\ \left(-D\nabla u + Vu\right)\cdot n_{in} = 0, & \forall x \in \partial\Omega_{in}, \text{ and } t > 0, \\ \nabla u \cdot n_{out} = 0, & \forall x \in \partial\Omega_{out}, \text{ and } t > 0, \end{cases} \tag{10}$$

where Ω is a bounded domain in $\mathbb{R}^n$ (where $1 \leq n \leq 3$) with a piecewise smooth boundary $\partial\Omega$. $D\left(x,t\right) \geq 0$ is the diffusion (dispersion) coefficient or the diffusivity. We suppose that $u\left(x,0\right) = u_0\left(x\right)$ for $x \in \Omega$, where u_0 is a continuous (or possibly discontinuous) function. Let $\partial\Omega_{in}$ and $\partial\Omega_{out}$ be partitions of the boundary $\partial\Omega$ where $\partial\Omega_{in}$ is the boundary at the inflow of mosquitoes in Ω and $\partial\Omega_{out}$ is the boundary at the outflow. n_{in} and n_{out} are respectively the unit outward normal to the boundaries Ω_{in} and Ω_{out}. We consider total flux Cauchy boundary conditions on $\partial\Omega_{in}$ [54], and Neumann boundary conditions on $\partial\Omega_{out}$. For sake of simplicity, we consider these conditions homogeneous.

Entomologists usually assume that there is no passive transportation of *Ae. albopictus* mosquito by the wind. Conversely, mosquitoes follow (or is looking for) odors and carbon dioxide (CO_2) carried by the wind [27], which gives a main direction of migration of mosquitoes; this is modeled by the term $\nabla\left(V\left(x,t\right)u\right)$. Since, we will only consider a time dependant V, we will simply write $V\nabla u$. Indeed, it is well known that CO_2, in interaction with other components, acts as an attractant and induces a direct response to guide the mosquito towards the host. The breeding sites or the blood feeding sites attractions are modeled by the term $\nabla\left(\nabla C\left(x,t\right)u\right)$, where $\nabla C(x,t)$ represents the force of attraction toward favorable "places". In C we will take into account wind direction and strength to determine the area of attraction, which is commonly called "plume" by entomologists. For the sake of simplicity, the effective attraction areas are represented by ellipses. The attractor function is set as one of the foci of the ellipse, and the other focus point is calculated as a function of the wind's direction and strength (Fig. 3, Eq. 11).

Outside the ellipse, there is no attraction and the related advection term is equal to zero. Note that if there is no wind, the attraction area is reduced to a disk of which the center is the attractor. Note also that our model could be coupled with a "plume" PDE model that has been published recently [14], where the authors consider an Individual Based Model approach to model a mosquito behavior (another mosquito species), according to the time and space evolution of the plume and the wind.

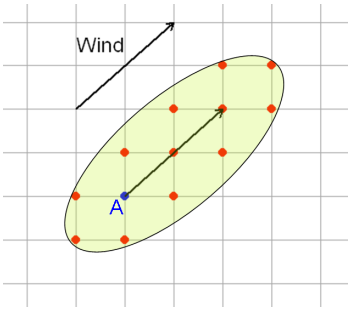

Figure 3: Construction of th ellipse of attraction with restect to wind's direction and strength.

The force of the attraction inside these areas are given by the following equations :

$$\nabla C(x,y) = \begin{pmatrix} C_{max} e^{-q\left((x-A_x)^2+(y-A_y)^2\right)} sign(x-A_x), \\ C_{max} e^{-q\left((x-A_x)^2+(y-A_y)^2\right)} sign(y-A_y), \end{pmatrix} \tag{11}$$

where (A_x, A_y) are the coordinates of attractor A, C_{max} is the maximum value reached when $(x,y) = (A_x, A_y)$, and q controls the amplitude between the minimum and maximum values taken by $C(x,y)$ in the attraction area. Moreover, the attraction sites are not localized near the border of the domain such that the areas of attraction do not encounter the border.

The reaction term $g(u,x,t)$ can be nonlinear, and represents death, birth, migration in the population. Because we only focus on mosquito dispersal, we may consider a linear $g(u,x,t) = -M(x)u + b(x,t)$, where M would be the mean daily death rate, and b would represent the birth rate in breeding sites.

Since we choose g linear, system (10) is a linear parabolic system. Thus it is possible to show the existence of a local solution [34].

Remark 3. *Chemical vector control can be considered in the reaction term, with additional terms in the mortality rates that may depend on the space*

variable, taking into account the fact that adulticides, for instance, have a limited area of efficacy.

Finally, we add a last parabolic equation related to the periodic releases of sterile males. We assume, for simplicity that dispersal ability of sterile males are similar to the wild ones. Note carefully that these releases will be done on various places on the domain, which implies a more complex equation.

3.3.1 The spatio-temporal compartmental model

According to the above explanations, we derive the following spatio-temporal model:

$$
\left\{
\begin{array}{rcl}
\frac{\partial u_A}{\partial t} & = & N_{Egg}(1-\frac{u_A}{K})\mathbf{1}_b u_b(x,t) - (\eta_A + M_A)u_A, \\
\frac{\partial u_Y}{\partial t} & = & \nabla(D\nabla u_Y) + V\nabla u_Y - (M_Y+\beta_Y)u_Y + r\eta_A u_A, \\
\frac{\partial u_f}{\partial t} & = & \nabla(D\nabla u_f) + V\nabla u_f - \nabla(\nabla C_f(x)u_f) - (M_f+\mu_{fr}\mathbf{1}_f)u_f \\
 & & +\mu_{bf}\mathbf{1}_b u_b + \beta_Y(\frac{u_M+\lambda_s f_s u_{Ms}}{u_M+u_{Ms}})u_Y, \\
\frac{\partial u_r}{\partial t} & = & \nabla(D\nabla u_r) + V\nabla u_r - (M_f+\mu_{rb})u_r + \mu_{fr}\mathbf{1}_f u_f, \\
\frac{\partial u_b}{\partial t} & = & \nabla(D\nabla u_b) + V\nabla u_b - \nabla(\nabla C_b(x)u_b) - (M_f+\mu_{bf}\mathbf{1}_b)u_b + \mu_{rb}u_r, \\
\frac{\partial u_M}{\partial t} & = & \nabla(D\nabla u_M) + V\nabla u_M - \nabla(\nabla C_f(x)u_M) - \nabla(\nabla C_b(x)u_M) \\
 & & -M_m u_M + (1-r)\eta_A u_A, \\
\frac{\partial u_{Ms}}{\partial t} & = & \nabla(D\nabla u_{Ms}) + V\nabla u_{Ms} - \nabla(\nabla C_f(x)u_{Ms}) - \nabla(\nabla C_b(x)u_{Ms}) - M_{ms}u_{Ms}, \\
u_A(x,0) = u_{A_0}(x), & & x\in\Omega, \\
u_X(x,0) = 0, & & x\in\Omega \text{ with } X\in\{Y,f,b,M,Ms\}, \\
(-D\nabla u_X + Vu_X)\cdot n_{in} = 0, & & \forall x\in\partial\Omega_{in}, \text{ and } t>0 \text{ with } X\in\{Y,f,r,b,M,Ms\}, \\
\nabla u_X\cdot n_{out} = 0, & & \forall x\in\partial\Omega_{out}, \text{ and } t>0, \text{ with } X\in\{Y,f,r,b,M,Ms\} \\
u_{Ms}(x,t_{start}+p\tau^+) = u_{Ms}(x,t_{start}+p\tau) + \Lambda_s\mathbf{1}_s(x), & & p=1,2,...,P
\end{array}
\right. \tag{12}
$$

After rescaling, we consider $\Omega = [-1,1]^2$, $Q_T = \Omega\times(0,T]$. We set three indicator functions, $\mathbf{1}_b$, $\mathbf{1}_f$ and $\mathbf{1}_s$. Function $\mathbf{1}_b$ defines the area where the breeding females may find a breeding site to lay eggs and become feeding females. $\mathbf{1}_f$ defines the area where feeding females may find a blood meal and become resting females. $\mathbf{1}_s$ defines the area where sterile males are released, with a periodicity τ, and $p = 0,\ 1,\ ...\ P$. The parameter C_f represents the attraction due to blood meals, like houses, and C_b represents the attraction due to the humidity coming from the breeding sites. Note that we assume that resting females are not subjected to the attraction of blood meals nor breeding site, they diffuse slowly, and their direction can be affected by the wind.

To provide numerical simulations of system (12), we need to construct a reliable algorithm, that preserves most of the properties of the system (positivity of the solution, equilibrium, if any, and its (un)stability properties).

3.4 Numerical Methods

There exists numerous methods to solve differential systems like system (12). However, we prefer to consider the operator splitting method [30] which consists of splitting a complex model into a sequence of simpler sub-models. First, because it is a very interesting approach that is not sufficiently used despite the fact that it is easy to implement, and offers flexibility to consider different appropriate numerical schemes to estimate each operator equation. Second, because the splitting method allows to use the nonstandard scheme, developed previously for the temporal model, to solve the reaction operator.

3.4.1 Splitting operator method

System (12) can be rewritten as follows:

$$u_t = f(x,u) = \mathcal{A}(u) + \mathcal{D}(u) + \mathcal{R}(u), \tag{13}$$

where $\mathcal{A}$ represents the advective terms, $\mathcal{D}$ the diffusive terms and $\mathcal{R}$ the reaction terms. The basic splitting operator method consists of solving successively the advective term, the diffusive term, and the reaction term, using the most efficient numerical method for each process.

Let $\Delta t > 0$ be the time-step, if we note u^n the approximation of u at a certain time t_n, then solving numerically the previous equation using the splitting approach leads to the following (formal) algorithm:

- solve $\frac{du_{\mathcal{A}}}{dt} = \mathcal{A}(u_{\mathcal{A}})$ with $u_{\mathcal{A}}(0) = u^n$ on $[0, \Delta t]$
- solve $\frac{du_{\mathcal{D}}}{dt} = \mathcal{D}(u_{\mathcal{D}})$ with $u_{\mathcal{D}}(0) = u_{\mathcal{A}}(\Delta t)$ on $[0, \Delta t]$,
- solve $\frac{du_{\mathcal{R}}}{dt} = \mathcal{R}(u_{\mathcal{R}})$ with $u_{\mathcal{R}}(0) = u_D(\Delta t)$,

then we set $u^{n+1} = u_{\mathcal{R}}(\Delta t)$.

In general, the splitting error is in $O(\Delta t^p)$ where p is the order of the splitting method (see [35] for examples). But in our case, since we consider linear operators, better results can be expected [35].

Each process equation is estimated using a well suited and simple scheme. The advection operator equation is estimated using the Corner Transport

Upwind (CTU) scheme developed by Collela [13] for the spatial discretization, and the time discretization is done using Euler's implicit scheme. For the diffusion equation, we consider a second order finite difference method for the spatial discretization, and the TR-BDF2 [29] method for the time discretisation. The TR-BDF2 scheme is second-order accurate, and L-stable, and thus, is particularly well suited for stiff problems. Finally, the reaction equation is estimated using the nonstandard finite difference scheme developed for the temporal model. Our splitting operator scheme permits to provide several simulations with and without constant parameters. Our following numerical simulations suggest that the solution converges, at least numerically, to a steady state.

4 Applications and simulations

We now provide several simulations, resulting from both the temporal and the spatio-temporal models. The algorithms are implemented in Scilab [48], and the figures are done using R [44]. For the temporal simulations, we tested the effect of temperature-varying parameters on the evolution of the number of mature females. In fact, in Réunion Island, the temperature is closely linked to the humidity which plays an important role in the abundance of mosquitoes. Thus, we need to distinguish the hot and rainy season from the cool and dry season. To do so, we used temperature data for the city of Saint-Denis, Réunion Island. Using SIT on a temperature-varying population, we assessed the importance of the period of the year at which SIT is done and may start. Spatio-temporal simulations permit to simulate even more strategies since it allows to take into account environmental components like heterogeneous landscape, wind, and mechanical control on targeted breeding sites....

To sterilize males, pupae were assumed to be irradiated at a dose of 35 Gy [41]. At this dose, the sterility is not total, and only $90 - 95\%$ of the sterile males would be totally sterile. Thus, we set $\lambda_s = 0.1$. According to Oliva & al. and co-authors ([41],[5]), with appropriate sugar supply, sterile males live on average 11.6 days, which implies $M_{ms} = 1/11.6$. The sexual competitivity is set as $f_s = 0.7$, [7]. In the following simulations, pulsed SIT is considered.

In the forthcoming simulations we will particularly study the abundance of mature females, $u_f + u_r + u_b$, which can be seen as a risk indicator for potential disease transmission.

4.1 Temporal model simulations

In Table 3, section 3.1.1, R_0 as well as the values at equilibrium are given for each compartment, at different temperatures. These values were evaluated using (2) and (3). We can observe that there are few females in the feeding compartment compared to the number of breeding and resting females. This can be explained by the fact that feeding essentially takes place in short time periods, in the morning and in the evening, in comparison to the time spent in the other compartments.

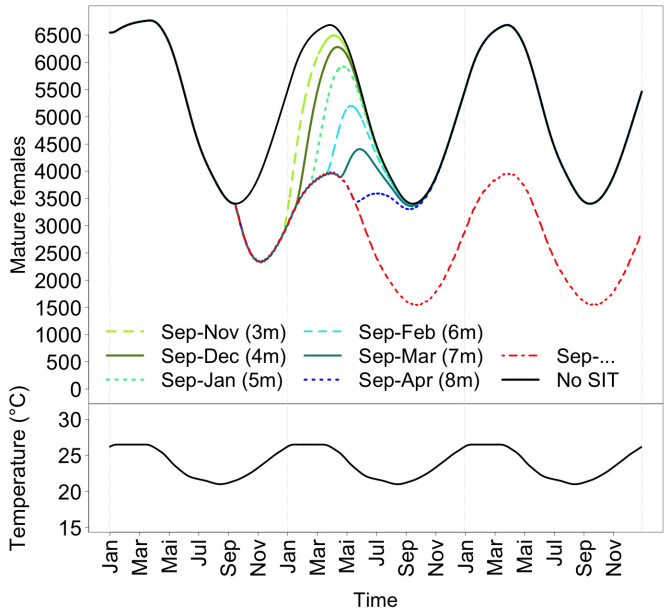

Figure 4: Evolution of the number of mature females, with SIT control with 7-days periodic releases of 2000 sterile males starting in September with releases durations varying from 3 months to 8 months. (Kmax=8000, f_s=0.7, $\rho_s = 1$).

In Fig. 4, we consider temperature-varying parameters. The temperature is an interpolation of the mean monthly temperatures of the city of Saint-Denis, Réunion Island. We assume that the experiment was carried out on a domain such that the maximum carrying capacity of the breeding sites is $K_{max} = 8000$. This figure shows the time evolution of the number of mature females over a period of 3 years, during which the temperature varies, with no vector control, and with SIT control of different durations. In agreement

with mark release recapture experiments [10] and field experts' knowledge, when there is no vector control (black curve), we observe that the mosquito population is larger at the end of the rainy season (end of March in Réunion Island) and lower at the end of the dry season (end of September).

Following the variation of the mosquito population along the year (Fig 4, black curve), it seems obvious to start the SIT control in September when the abundance of mosquitoes is low. In Fig. 4, the SIT consists of releases of 2000 sterilized males every 7 days, that start in September, but over period of time that varies from 3 months (light green dotted line) to 8 months (blue dotted line). The evolution of the abundance of mature females for SIT starting in September over an unlimited period of time is also represented (red dotted line). Figure 4 shows that the duration of SIT control is important: in fact, only a seven or an eight months treatment seems appropriate to keep the mosquito population at a low level. Obviously as soon as the SIT stops, the solution converges quickly to the periodic equilibrium (in black).

In these simulations the quality of the releases was assumed to be optimal with $\rho_s = 1$. However, if we assume that the releases are not optimal, for instance if we assume that the sterilized males are released far from the females, $\rho_s < 1$, then the number of sterile males released has to be multiplied by $1/\rho_s$ to obtain the same results as the optimal releases. For instance, if $\rho_s = 0.2$, we would need to release 10000 sterile males to obtain the same results as in Fig. 4.

4.2 Spatio-temporal simulations

For the spatio-temporal simulations we consider a squared domain of 200m $\times$ 200m, rescaled on [-1,1] $\times$ [-1,1]. This domain is inspired from the field where mark release recapture experiments have been conducted (see Fig 18). Five blood-feeding sites and eight breeding sites are distributed as in Fig 5(a). This layout is arbitrary and is not to be linked with any concrete experiment.

We assume that all attractors are similar: the same area of attraction, the same force of attraction. Let us recall that an area of attraction is represented as an ellipse for which the shape depends on the wind's direction and strength. Also, without wind, this area is reduced to a disk centered at the attractor's position. In agreement with field experts and/or based on field experiments [33], we set D=0.04$m^2 s^{-1}$, V=0.1 ms^{-1}, and C_{max}=1 ms^{-1}.

In SIT spatio-temporal simulations, sterile males are released periodically near the breeding sites such that they can mate with immature females immediately after emergence. Under this condition, the quality of the releases

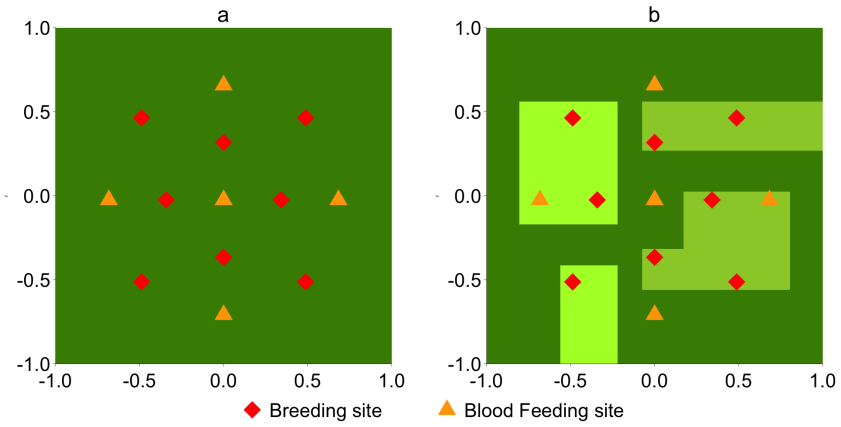

Figure 5: Distribution of the breeding sites and of the blood-feeding sites on a (a) homogeneous domain (b) heterogeneous domain (colored patches are related to different vegetation patterns)

is assumed to be optimal. The sexual competitivity is set as $f_s = 0.7$, [7].

4.2.1 Influence of the landscape. Simulations with constant parameters

We consider constant parameters related to a temperature of $25°C$. Fig. 6, shows the distribution of mature females at equilibrium on the homogeneous landscape (Fig. 5(a)), without wind and without vector control. At equilibrium, mature females gather around the breeding sites and the blood-feeding sites. When North wind is added, mature females migrate North as they trace back odors or CO_2 carried by the wind, and gather around the Northern attractors (see Fig. 7), preferably around blood-feeding sites than breeding sites. This is due to the fact that after they have taken their blood meal, resting females diffuse slowly around their hosts without being submitted to attraction.

Since mechanical control and SIT are simultaneously considered, with and without wind, the spatial distribution of the mosquito changes as well as the number of mature females. Here and later in the paper, mechanical control consists in removing the three South breeding sites and SIT consists in weekly releases of 2000 sterile males near the remaining breeding sites (see Fig. 8). This vector control allows to reduce the number of females who gather around the remaining attractors. Females are mostly present in the North, since the South breeding sites have been destroyed. When

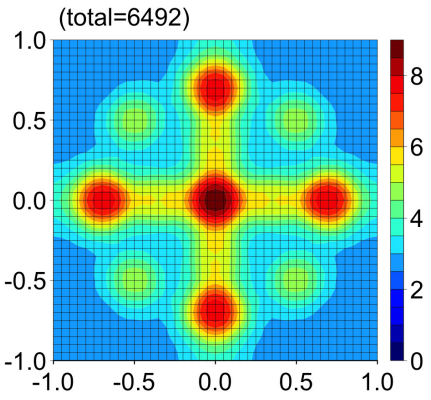

Figure 6: Distribution the mature females on a homogeneous landscape at $25°C$ without wind, with Kmax=1000 for each breeding sites (total Kmax=$8 \times 1000 = 8000$)

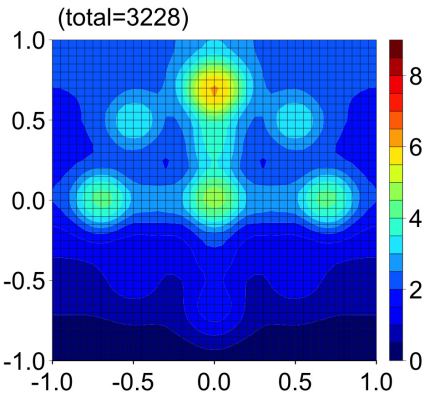

Figure 7: Distribution the mature females on a homogeneous landscape at $25°C$ with North wind, with Kmax=1000 for each breeding sites (total Kmax=$8 \times 1000 = 8000$)

North wind is considered, females migrate North and are therefore mostly distributed around the unique North blood-feeding site (see Fig. 9).

Despite the lack of studies about the impact of landscape on mosquito dispersal, it is most than probable that it can influence their displacements in terms of diffusion and advection. Indeed, it is believed that vegetation hedges may act as corridors, which would influence the directions of mosquito displacement [33]. Because of a lack of informations, we consider heterogeneity in landscape only in terms of diffusion. We may assume that the areas where the diffusion is lower correspond to areas "favorable" for the mosquito, where it will spend more time than elsewhere. Figure 5(b) is an example of heterogeneous landscape on which we define areas where the diffusivity is lower than anywhere else. We assume that the diffusivity in the left rectangles is multiplied by 0.05, whereas the diffusivity in the right polygons is multiplied by 0.1. With this layout, the breeding sites are located in areas where the diffusivity is low. We can assume they are located in bushes for example. Three hosts, i.e. feeding sites, are outside the low diffusion areas of, while the two others (the East and West hosts), are inside the low diffusion areas.

Whithout vector control, mature females tend to gather around the at-

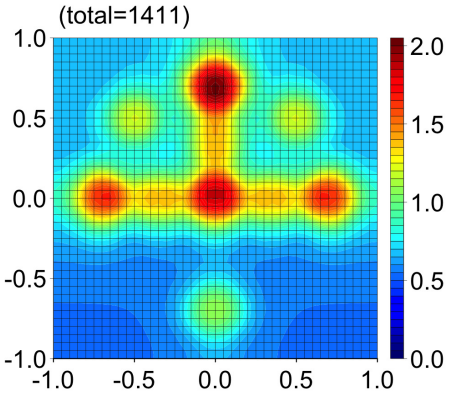

Figure 8: Distribution the mature females on a homogeneous landscape at $25°C$ without wind, with destruction of the 3 South breeding sites, with Kmax=1000 for each remaining breeding sites (total Kmax=$5 \times 1000 = 5000$) and SIT with 7-days periodic releases of 2000 sterile males near the remaining breeding sites, with $f_s = 0.7$.

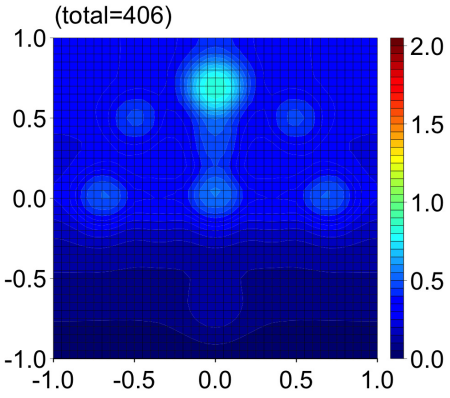

Figure 9: Distribution the mature females on a homogeneous landscape at $25°C$ with North wind, with destruction of the 3 South breeding sites, with Kmax=1000 for each remaining breeding sites (total Kmax=$5 \times 1000 = 5000$) and SIT with 7-days periodic releases of 2000 sterile males near the remaining breeding sites, with $f_s = 0.7$

tractors located in the areas with low diffusivity, as expected. Thus peaks are observed around the West host and its neighboring breeding site (see Fig. 10). Once again, as North wind is added, a North migration of the population can be observed (Fig. 11): the peaks still hold, but the mature females population is smaller.

In Figs. 12 and 13, like in the previous simulations, we consider simultaneously mechanical and SIT controls, without wind and with North wind, respectively. Once again, the effect of vector control is visible since it allows to reduce the abundance of females who are now essentially present in the upper part of the domain due to the destruction of the 3 South breeding sites.

Altogether, the previous simulations show that the landscape heterogeneity, and in some sense the vegetation, does really play an important role in the dispersal of mosquitoes. From a practical point of view, it may be useful

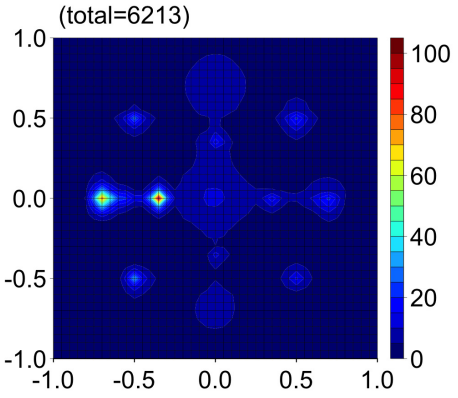

Figure 10: Distribution the mature females on a heterogeneous landscape at $25°C$ without wind, with Kmax=1000 for each remaining breeding sites.

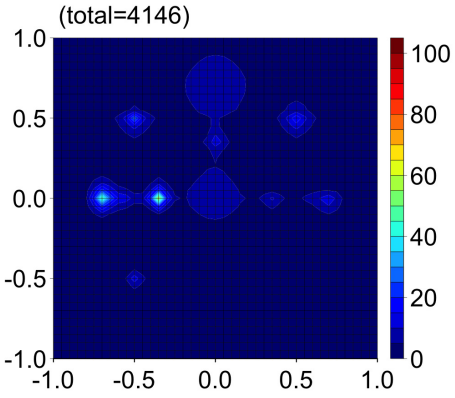

Figure 11: Distribution the mature females on a heterogeneous landscape at $25°C$ with North wind, with Kmax=1000 for each remaining breeding sites.

to know how mosquitoes are distributed on a domain, in order to determine where they are likely to gather, before conducting vector control. Our simulations show that when we consider an homogeneous landscape, with equal diffusion everywhere, females gather mostly around the hosts, Fig. 6 and Fig. 7. But, when we consider heterogeneous landscape with areas with different diffusion (advection) parameters, we observe a drastic change in the distribution. In this case, females are mostly present around the attractors located in the low-diffusion areas (see Figs. 10 and 11). Thus, in order to establish efficient vector control strategies, it is essential to take into account environmental factors, like the wind, landscape heterogeneity, and vegetation-mosquito interactions.

Assuming T_0 and T_c be respectively the total number of mature females without and with vector control, we can define the efficacy of a control strategy as follows: $E_c = (T_0 - T_c)/T_c$. Thus $E_c \in [0, 1]$: the larger E_c is, the more efficient the control strategy is. We summarize the previous simulations in Tab. 4, and provide some efficacy estimates. It seems obvious that the results, with North wind, are more contrasted between homogeneous and heterogeneous landscapes. This is partly due to the fact that during a windy period, mosquitoes hide in the vegetation protecting themselves from the wind.

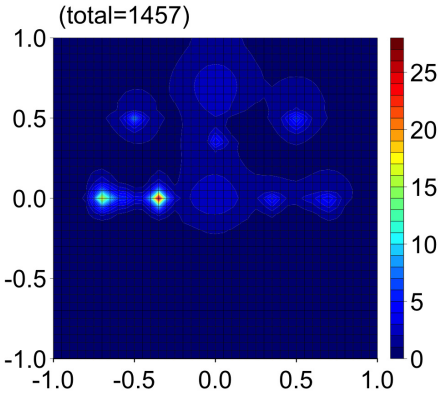

Figure 12: Distribution the mature females on a heterogeneous landscape at $25°C$ without wind, with destruction of the 3 South breeding sites, with Kmax=1000 for each remaining breeding sites and SIT with 7-days periodic releases of 2000 sterile males near the remaining breeding sites.

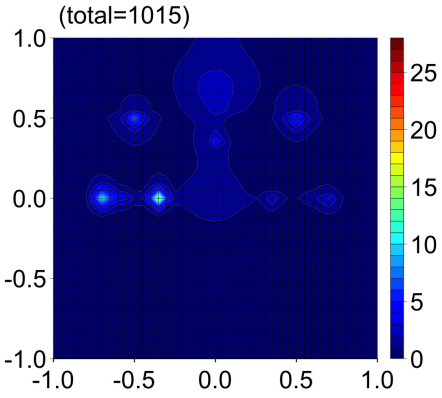

Figure 13: Distribution the mature females on a heterogeneous landscape at $25°C$ with North wind, with destruction of the 3 South breeding sites, with Kmax=1000 for each remaining breeding sites and SIT with 7-days periodic releases of 2000 sterile males near the remaining breeding sites.

4.2.2 SIT release strategies. Simulations with constant parameters

We compare two spatial strategies with two frequency strategies for the releases of sterile males on a homogeneous landscape, with North wind. We first consider weekly releases of 2000 sterile males, first near the 3 North breeding sites (Fig. 14), and then near the 3 South breeding sites (Fig. 15). Then, these results are compared to 28-days releases of 8000 sterilized males near the 3 North breeding sites and near the 3 South breeding sites, such that in all cases a total of 8000 sterile males are released over a period of 28 days.

According to the SIT releases strategy, the number of mature females on the domain is very different. The efficacies, E_S and E_N, have been calculated for respectively the South and the North releases strategy. Comparing

Environment		No Control	Control	Efficacy of Control
No Wind	Homogeneous	6492	1411	0.78
	Heterogeneous	6213	1457	0.77
North Wind	Homogeneous	3228	406	0.87
	Heterogeneous	4146	1015	0.76

Table 4: Comparison of efficacy of control with respect to different environment conditions (wind and landscape). The control consists of the destruction of the 3 South breeding sites along with 7-days periodic releases of 2000 sterilized males near the 5 remaining breeding sites. ($\Lambda_s = 2000$, Period=7 days, $\lambda_s = 0.1$, $f_s = 0.7$)

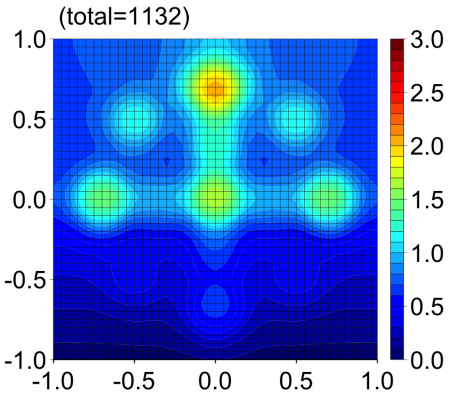

Figure 14: Distribution the mature females on a homogeneous landscape at $25°C$ with North wind, with SIT: 7-days periodic releases of 2000 sterile males near the North breeding sites

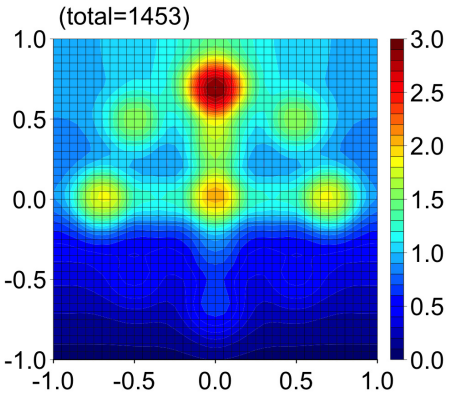

Figure 15: Distribution the mature females on a homogeneous landscape at $25°C$ with North wind, with SIT: 7-days periodic releases of 2000 sterile males near the South breeding sites

Figs.14 and 15, it is obvious that releases near the North breeding sites (upwind) is more efficient, with $E_N = 0.65$, than releases near the South breeding sites (downwind), with $E_S = 0.55$. This can be explained by the fact that most of the females have moved to the North due to North wind. Naturally, SIT is more efficient if the sterilized males are released in places where there are already a lot of females. In our case, it is the North of the domain. Therefore, in order to optimize the impact of SIT, it is important to have an accurate estimate of the distribution of the wild females, and for

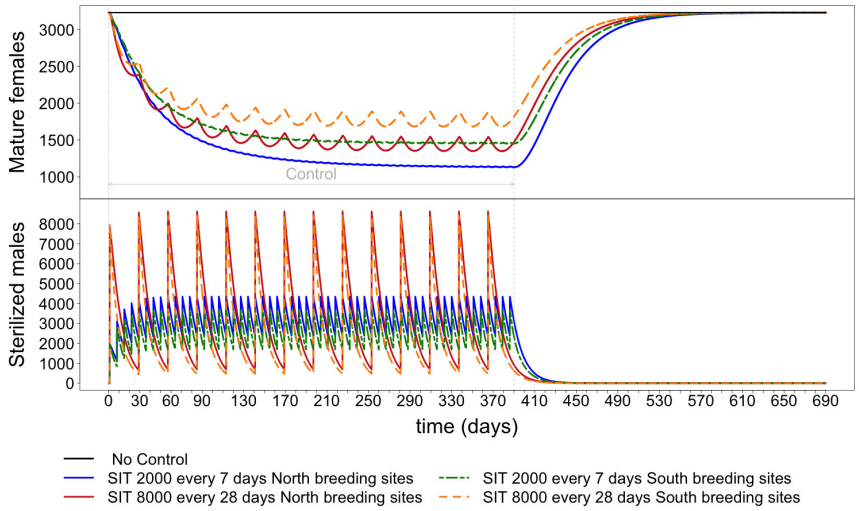

Figure 16: Time evolution of the number of mature females (top) and of the number of sterile males (bottom) on a homogeneous landscape with North wind. Two spatial strategies: releases of sterile males near the 3 North breeding sites vs. releases near the South breeding sites, with $f_s = 0.7$. Two frequency strategies are considered: 7-day periodic releases of 2000 sterile males vs. 28-day periodic releases of 8000 sterile males.

that reason it is important to take into account the environmental data. Moreover, comparing two frequency strategies for North and South releases (Fig. 16), small and frequent releases turned out to be more efficient than bigger and less frequent releases.

4.2.3 SIT with Temperature-varying parameters

We now consider an impulse spatio-temporal SIT control with weekly releases of 2000 sterile males near the 3 North breeding sites on a homogeneous landscape, with North wind. In Fig. 17(a), we consider a SIT control duration from 3 to 6 months. As a result, in this case, SIT over a period of 3 months starting in September is clearly not long enough. By the end of the treatment, the environmental conditions are still too favorable for the biological development of *Aedes*, which makes the population grow towards the initial periodic equilibrium as soon as the treatment stops. And thus, the population peak is not avoided. However, SIT over a period of 6 months is more

efficient: the period and the duration of SIT control is part of the success of SIT. Under the same environmental conditions, in Fig. 17(b), we present

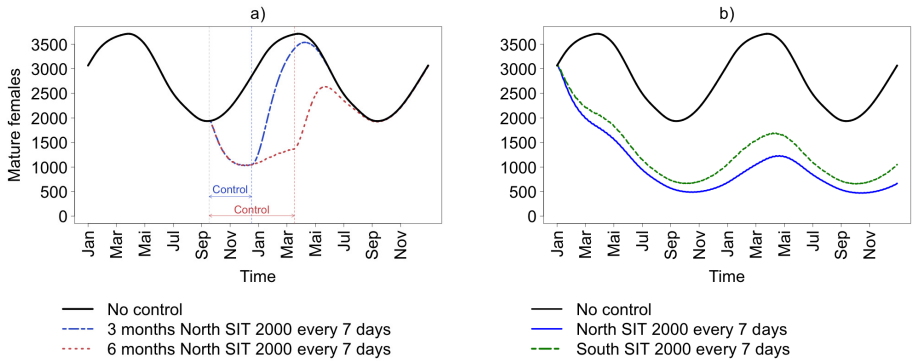

Figure 17: Time evolution of the number of mature females on a homogeneous landscape with North wind, with temperature-varying parameters, with weekly SIT releases of 2000 sterile males near the South breeding sites starting for durations of 3 months and 6 months (a), permanent SIT control (b)

results of weekly releases of 2000 sterilized males near the 3 North breeding sites (blue line) and near the 3 South breeding sites (green dotted line) over an unlimited period of time. The decay in the mosquito population is significative: we reach a new periodic equilibrium with a lower peak (50% lower than without SIT control). Lower values could be reached if we were able to release sterile males near all other breeding sites or if the releases were larger. Of course, if, for any reason, SIT control stops, then the mosquito population will reach the no-control periodic equilibrium.

5 Conclusion

Ae. albopictus is geographically established in most parts of the world and is considered as the principal vector of many vector-borne diseases, like chikungunya, dengue, or yellow fever. This implies that outbreaks are not ruled-out, and the risk for potential epidemics poses a threat for public health. Methods such as mechanical control and the use of adulticides and larvicides are useful, but cannot be of long time use. In Réunion Island, a biodiversity hotspot, with mountainous landscape, the use of chemical products is limited because of its detrimental effect on environment and some endemic

species. New sustainable tools, like the Sterile Insect Technique could be an interesting alternative as control tool. In order to pretend to develop SIT sucessfully, a lot of knowledges on the biology and ecology of *Ae. albopictus* are needed, but also accurate modeling of the population spatio-temporal dynamics. These models will be helpful to conduct experiments or to verify/validate hypotheses with a minimal number of real experiments, that can be very complex and expensive.

The models developed in the present work are linked to one of the models developed and studied in [23], with some modifications and improvements. We have first considered a temporal compartimental approach and then include the spatial component that leads to a system of coupled diffusion-advection-reaction-like equations to model mosquito dispersal. For the latter, the technique of operator splitting has been considered to construct a reliable and fast algorithm, using appropriate numerical methods to solve each operator. The main point here was not to use sophisticated and the most accurate schemes, but, preferably easy-to-implement and fast schemes. Our study is mainly qualitative rather than quantitative. However our results are not too far from real measurements using Mark-Release-Recapture (MRR) experiments [33].

The numerical simulations assessed the importance of a certain number of environmental factors that can potentially affect the efficiency of SIT on a temporal, and spatio-temporal scale. The value of the temperature, for instance, affects directly the dynamics of the mosquito population. We saw that the number of females at equilibrium is largely affected by the temperature. We simulated the evolution of the population with annual variations of the temperature using data for the city of Saint-Denis, the main city of Réunion Island. We observed that mosquitoes are more abundant at the end of the hot and rainy season, and less abundant at the end of the cool and dry season. This is an important fact to take into account when releasing sterile males. The duration of the SIT treatment is also essential. If SIT starts when the abundance of females is low, then the treatment must last long enough to keep the female mosquitoes below a certain threshold. The frequency and number of sterile males released must also be taken into consideration for optimizing SIT. We confirm and enhance to a spatio-temporal model the result of Dumont and Tchuenche [23] as we showed that, in the case of pulsed releases, it would be more efficient to consider smaller and more frequent releases rather than bigger and less frequent releases [53].

It is obvious that landscape parameters have also a strong impact on SIT strategies. Vegetation patches or landscape elements, for instance, that favor

or not mosquito dispersal, can have a strong influence in mosquito distribution, and thus on the locations of the SIT releases. The interactions between mosquitoes and vegetation deserve further investigations to understand exactly how landscape elements influence the displacements of *Ae. albopictus*. This is mandatory to be able to consider a vector map, like Fig. 18 which represents our MRR experimental site and take into account different landscape elements, like houses, gardens, hedges, sugar cane fields, for which our model needs to be parameterized, in order to make valuable numerical simulations. Finally, the wind is another non-negligible factor to take into account for the success of SIT as it affects directly the spatial distribution of mosquitoes. It has an advective role, it is essential to have a good estimate of the areas of high abundance of females in order to better target the SIT releases, Tab. 4.

Finally, further works could be done from the mathematical and computational point of view. For instance, the existence of a solution of the impulse parabolic system (12) could be considered, as well as the existence of a periodic equilibrium. Then, in order to take into account more precisely environmental and landscape parameters, High Performance Computing and more accurate numerical schemes should be considered or developed, like, for instance, WENO methods to solve the advective term [49].

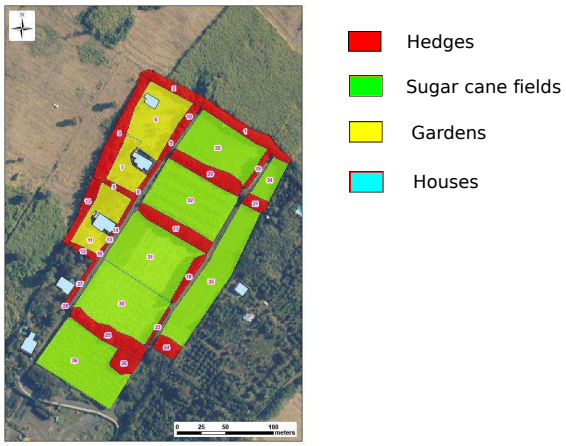

Figure 18: Vector map of the experimental site [36].

Acknowlegments

C. Dufourd and Y. Dumont have been partially supported by the "SIT feasibility programme" in Reunion, jointly funded by the French Ministry of Health and the European Regional Development Fund (ERDF). The authors would like to thank the reviewers for valuable and constructive remarks that helped greatly to improve the paper.

References

[1] R. Anguelov, Y. Dumont, and J. Lubuma. Mathematical modeling of sterile insect technology for control of anopheles mosquito. Computers and Mathematics with Applications, **64**(3):374–389, 2012.

[2] R. Anguelov, Y. Dumont, J. Lubuma, and E. Mureithi. Stability analysis and dynamics preserving non-standard finite difference schemes for a malaria model. to appear in Mathematical Population Studies., 2013.

[3] R. Anguelov, Y. Dumont, and J. M.-S. Lubuma. On nonstandard finite difference schemes in biosciences. AIP Conference Proceedings, **1487**(1):212–223, 2012.

[4] R. Anguelov, Y. Dumont, J. M.-S. Lubuma, and M. Shillor. Dynamically consistent nonstandard finite difference schemes for epidemiological models. Technical Report UPWT2009/22, University of Pretoria, 2009.

[5] F. Balestrino, A. Medici, G. Candini, M. Carrieri, B. Maccagnani, M. Calvitti, S. Maini, and R. Bellini. gamma Ray Dosimetry and Mating Capacity Studies in the Laboratory on Aedes albopictus Males. Journal of medical entomology, **47**(4):581–591, JUL 2010.

[6] H.J. Barclay. Mathematical models for the use of sterile insects. In V.A. Dyck, J. Hendrichs, and A.S. Robinson, editors, Sterile Insect Technique, pages 147–174. Springer Netherlands, 2005.

[7] R. Bellini, M. Calvitti, A. Medici, M. Carrieri, G. Celli, and S. Maini. Use of the sterile insect technique against aedes albopictus in italy: First results of a pilot trial. Area-Wide Control of Insect Pests, pages 505–515, 2007.

[8] M.Q. Benedict, R.S. Levine, W.A. Hawley, and L.P. Lounibos. Spread of the tiger: global risk of invasion by the mosquito aedes albopictus. Vector-Borne and Zoonotic Diseases, **7**(1):76–85, 2007.

[9] S. Bowong, Y. Dumont, and Jean-Jules Tewa. A patchy model for chikungunya-like diseases. Submitted.

[10] S. Boyer, J.S. Dehecq, G. Lemperiere, and Y. Dumont. Sample method to estimate the size of adult mosquito population: study case of aedes albopictus in la reunion island. 2012. submitted.

[11] S. Boyer, J. Gilles, D. Merancienne, G. Lemperiere, and D. Fontenille. Sexual performance of male mosquito aedes albopictus. Medical and Veterinary Entomology, **25**:454–459, 2011.

[12] A.N. Clements. The Biology of Mosquitoes: Development, nutrition, and reproduction. The Biology of Mosquitoes. Chapman & Hall, 1992.

[13] P. Colella. Multidimensional upwind methods for hyperbolic conservation laws. Journal of Computational Physics, **87**(1):171–200, 1990.

[14] B. Cummins, R. Cortez, I.M/ Foppa, J. Walbeck, and J.M Hyman. A spatial model of mosquito host-seeking behavior. PLoS computational biology, 8(5):e1002500, 2012.

[15] P.N. Daykin, F.E. Kellogg, and R.H. Wright. Host-finding and repulsion of aedes aegypti. The Canadian Entomologist, **97**(3):239–263, 1965.

[16] H. Delatte, G. Gimonneau, A. Triboire, and D. Fontenille. Influence of temperature on immature development, survival, longevity, fecundity, and gonotrophic cycles of aedes albopictus, vector of chikungunya and dengue in the indian ocean. Journal of medical entomology, **46**(1):33–41, 2009.

[17] H. Delatte, C. Paupy, J.S. Dehecq, J. Thiria, A.B. Failloux, D. Fontenille, et al. Aedes albopictus, vector of chikungunya and dengue viruses in reunion island: biology and control. Parasite (Paris, France), **15**(1):3, 2008.

[18] C. Dufourd and Y. Dumont. Modeling and simulations of mosquito dispersal. the case of aedes albopictus. BIOMATH, **1**(2):Article–ID, 2012.

[19] Y. Dumont and F. Chiroleu. Vector control for the chikungunya disease. Mathematical Biosciences and Engineering, **7**(2):313–345, 2010.

[20] Y. Dumont, F. Chiroleu, and C. Domerg. On a temporal model for the chikungunya disease: Modeling, theory and numerics. Mathematical biosciences, **213**(1):80–91, 2008.

[21] Y. Dumont and C Dufourd. Spatio-temporal modeling of mosquito distribution. In AIP Conference Proceedings-American Institute of Physics, volume **1404**, pages 162–165, 2011.

[22] Y. Dumont, R. Russel, V. Lecomte, and M. Le Corre. Conservation of endangered endemic seabirds within a multi-predator context: the barau's petrel in réunion island. Natural Resource Modelling, **23**(3):381–436, 2010.

[23] Y. Dumont and J.M. Tchuenche. Mathematical studies on the sterile insect technique for the chikungunya disease and *Aedes albopictus*. Journal of Mathematical Biology, **65**(5):809–855, 2012.

[24] Yves Dumont and Jean M.-S. Lubuma. Non-standard finite-difference methods for vibro-impact problems. Proceedings of the Royal Society A: Mathematical, Physical and Engineering Science, **461**(2058):1927–1950, 2005.

[25] Lorenzo Farina and Sergio Rinaldi. Positive linear systems. Pure and Applied Mathematics (New York). Wiley-Interscience, New York, 2000. Theory and applications.

[26] F.N. Fritsch and R.E. Carlson. Monotone piecewise cubic interpolation. SIAM Journal on Numerical Analysis, pages 238–246, 1980.

[27] MT Gillies et al. The role of carbon dioxide in host-finding by mosquitoes (diptera: Culicidae): a review. Bulletin of Entomological Research, **70**:525–532, 1980.

[28] NG Gratz. Critical review of the vector status of Aedes albopictus. Medical and Veterinary Entomology, **18**(3):215–227, SEP 2004.

[29] M.E. Hosea and L.F. Shampine. Analysis and implementation of tr-bdf2. Applied Numerical Mathematics, **20**(1):21–37, 1996.

[30] W.H. Hundsdorfer and J.G. Verwer. Numerical solution of time-dependent advection-diffusion-reaction equations, volume **33**. Springer Verlag, 2007.

[31] Alberto Isidori. Nonlinear control systems. II. Communications and Control Engineering Series. Springer-Verlag London Ltd., London, 1999.

[32] E.F. Knipling. Sterile-Male Method of Population Control. Science, **130**(3380):902–904, 1959.

[33] R. Lacroix, H. Delatte, T. Hue, and P. Reiter. Dispersal and survival of male and female aedes albopictus (diptera: Culicidae) on reunion island. Journal of medical entomology, **46**(5):1117–1124, 2009.

[34] O.A. Ladyžhenskaya, V.A. Solonnikov, and N.N. Ural'tseva. Linear and Quasi-linear Equations of Parabolic Type, volume 23. Amer Mathematical Society, 1968.

[35] D. Lanser and J. G. Verwer. Analysis of operator splitting for advection-diffusion-reaction problems from air pollution modelling. Journal of Computational and Applied Mathematics, **111**(1-2):201–216, 1999. Numerical methods for differential equations (Coimbra, 1998).

[36] G. Lemperiere, J.S.. Boyer, S. Dehecq, C. Dufourd, and Y. Dumont. Influence of rural landscape structures on the dispersal of the asian tiger mosquito *Aedes albopictus* : a study case at la reunion island. 8th IALE (International Association of Landscape Ecology) World Congress, Beijing, China, August 18-23, 2011.

[37] M.A. Lewis and P. Van Den Driessche. Waves of extinction from sterile insect release. Mathematical Biosciences, **116**(2):221 – 247, 1993.

[38] V S Manoranjan and P Van Den Driessche. On a diffusion model for sterile insect release. Mathematical Biosciences, **79**:199–208, 1986.

[39] R.E. Mickens. Nonstandard finite difference models of differential equations. World Scientific Pub Co Inc, 1994.

[40] Clelia F. Oliva, Maxime Jacquet, Jeremie Gilles, Guy Lemperiere, Pierre-Olivier Maquart, Serge Quilici, François Schooneman, Marc J. B. Vreysen, and Sebastien Boyer. The sterile insect technique for controlling populations of *Aedes albopictus* (diptera: Culicidae) on reunion island: Mating vigour of sterilized males. PLoS ONE, 7(11):e49414, 11 2012.

[41] Clelia F. Oliva, Marco J. Maier, Jeremie Gilles, Maxime Jacquet, Guy Lemperiere, Serge Quilici, Marc J.B. Vreysen, François Schooneman,

Dave D. Chadee, and Sebastien Boyer. Effects of irradiation, presence of females, and sugar supply on the longevity of sterile males aedes albopictus (skuse) under semi-field conditions on reunion island. Acta Tropica, **125**(3):287 – 293, 2013.

[42] C. Paupy, H. Delatte, L. Bagny, V. Corbel, and D. Fontenille. Aedes albopictus, an arbovirus vector: From the darkness to the light. Microbres And Infection, **11**(14-15):1177–1185, DEC 2009.

[43] Christophe Paupy, Benjamin Ollomo, Basile Kamgang, Sara Moutailler, Dominique Rousset, Maurice Demanou, Jean-Pierre Herve, Eric Leroy, and Frederic Simard. Comparative Role of Aedes albopictus and Aedes aegypti in the Emergence of Dengue and Chikungunya in Central Africa. Vector-Borne and Zoonotic Diseases, **10**(3):259–266, APR 2010.

[44] R Development Core Team. R: A Language and Environment for Statistical Computing. R Foundation for Statistical Computing, Vienna, Austria, 2011. `http://www.R-project.org/`.

[45] R Ross. The relationship of malaria and the mosquito . Lancet, **2**:48–50, 1900.

[46] R Ross. Malaria and mosquitoes. Nature, **63**:440, NOV-APR 1901.

[47] R Ross. The possibility of reducing mosquitoes. Nature, **72**:151, MAY-OCT 1905.

[48] Scilab Enterprises. Scilab: Le logiciel open source gratuit de calcul numérique. Scilab Enterprises, Orsay, France, 2012. `http://www.scilab.org`.

[49] Chi-Wang Shu. High order weighted essentially nonoscillatory schemes for convection dominated problems. SIAM Review, **51**(1):82–126, 2009.

[50] João Teixeira and Maria João Borges. Existence of periodic solutions of ordinary differential equations. Journal of Mathematical Analysis and Applications, **385**(1):414 – 422, 2012.

[51] R. Varga. Matrix Iterative Analysis. Prentice-Hall, Prentice Hall, Englewoods Cliffs, NJ, 1962.

[52] M. Vidyasagar. Decomposition techniques for large-scale systems with nonadditive interactions: stability and stabilization. IEEE Transaction on Automatic Control, **25**:773–779, 1980.

[53] S. M. White, P. Rohani, and S. M. Sait. Modelling pulsed releases for sterile insect techniques: fitness costs of sterile and transgenic males and the effects on mosquito dynamics. Journal of Applied Ecology, 2010.

[54] A. Younes and P. Ackerer. Solving the advection-diffusion equation with the eulerian–lagrangian localized adjoint method on unstructured meshes and non uniform time stepping. Journal of Computational Physics, **208**(1):384–402, 2005.

A Proof of Proposition 2

We compute the Jacobian matrix of system (1): $J(u) =$

$$\begin{pmatrix} -(\eta_A + M_A + \frac{N_{Egg}u_b}{K}) & 0 & 0 & 0 & N_{Egg}\left(1-\frac{u_A}{K}\right) & 0 \\ r\eta_A & -(M_Y+\beta_Y) & 0 & 0 & 0 & 0 \\ 0 & \beta_Y & -(M_f+\mu_{fr}) & 0 & \mu_{bf} & 0 \\ 0 & 0 & \mu_{fr} & -(M_f+\mu_{rb}) & 0 & 0 \\ 0 & 0 & 0 & \mu_{rb} & -(M_f+\mu_{bf}) & 0 \\ (1-r)\eta_A & 0 & 0 & 0 & 0 & -M_m \end{pmatrix}.$$

Thus, taking $u = \mathbf{0}$, we deduce

$$J(\mathbf{0}) = \begin{pmatrix} -(\eta_A + M_A) & 0 & 0 & 0 & N_{Egg} & 0 \\ r\eta_A & -(M_Y+\beta_Y) & 0 & 0 & 0 & 0 \\ 0 & \beta_Y & -(M_f+\mu_{fr}) & 0 & \mu_{bf} & 0 \\ 0 & 0 & \mu_{fr} & -(M_f+\mu_{rb}) & 0 & 0 \\ 0 & 0 & 0 & \mu_{rb} & -(M_f+\mu_{bf}) & 0 \\ (1-r)\eta_A & 0 & 0 & 0 & 0 & -M_m \end{pmatrix}.$$

This is again a Metzler matrix that admits a regular splitting $J(\mathbf{0}) = N + M$, where $N = diag(J(\mathbf{0}))$, and

$$M = \begin{pmatrix} 0 & 0 & 0 & 0 & N_{Egg} & 0 \\ r\eta_A & 0 & 0 & 0 & 0 & 0 \\ 0 & \beta_Y & 0 & 0 & \mu_{bf} & 0 \\ 0 & 0 & \mu_{fr} & 0 & 0 & 0 \\ 0 & 0 & 0 & \mu_{rb} & 0 & 0 \\ (1-r)\eta_A & 0 & 0 & 0 & 0 & 0 \end{pmatrix}.$$

Let us recall that $\alpha(J(\mathbf{0})) < 0$ if and only if $\rho(-N^{-1}M) < 1$ [22, 51], where $\rho(A)$ denotes the spectral radius of A and $\alpha(A)$ denotes the stability modulus

of A. Thus, we have

$$-N^{-1}M = \begin{pmatrix} 0 & 0 & 0 & 0 & \frac{N_{Egg}}{\eta_A+M_A} & 0 \\ \frac{r\eta_A}{M_Y+\beta_Y} & 0 & 0 & 0 & 0 & 0 \\ 0 & \frac{\beta_Y}{M_f+\mu_{fr}} & 0 & 0 & \frac{\mu_{bf}}{M_f+\mu_{fr}} & 0 \\ 0 & 0 & \frac{\mu_{fr}}{M_f+\mu_{rb}} & 0 & 0 & 0 \\ 0 & 0 & 0 & \frac{\mu_{rb}}{M_f+\mu_{bf}} & 0 & 0 \\ \frac{(1-r)\eta_A}{M_m} & 0 & 0 & 0 & 0 & 0 \end{pmatrix}.$$

Straightforward computations show that $\rho(-N^{-1}M) < 1$ if and only if $R_0 < 1$. Thus, we deduce that TE is LAS when $R_0 < 1$ and unstable otherwise.

We then consider the Jacobian computed at E:

$$J(E) = \begin{pmatrix} -(\eta_A + M_A + \frac{N_{Egg}}{K}u_b^*) & 0 & 0 & 0 & \frac{N_{Egg}}{R_0} & 0 \\ r\eta_A & -(M_Y+\beta_Y) & 0 & 0 & 0 & 0 \\ 0 & \beta_Y & -(M_f+\mu_{fr}) & 0 & \mu_{bf} & 0 \\ 0 & 0 & \mu_{fr} & -(M_f+\mu_{rb}) & 0 & 0 \\ 0 & 0 & 0 & \mu_{rb} & -(M_f+\mu_{bf}) & 0 \\ (1-r)\eta_A & 0 & 0 & 0 & 0 & -M_m \end{pmatrix},$$

$J(E)$ being again a Metzler matrix we use the same approach than before. Direct computations, show that E is LAS when $R_0 > 1$.

B Proof of Theorem 1

We first show that TE is globally asymptotically stable. It is obvious that system (1) can be rewritten as two subsystems

$$\begin{cases} \frac{dx}{dt} = f(x) = A(x)x, \\ \frac{dy}{dt} = g(x,y) \end{cases}$$

where $x = (u_A, u_Y, u_f, u_r, u_b)^T$, and $y = u_M$. Let us first show that $\mathbf{0}_5$ is a GAS equilibrium of system $\frac{dx}{dt} = f(x) = A(x)x$.

It suffices to consider the following Lyapunov function $V(x) =< W, x >$, with

$$W = \left(1, \frac{(\eta_A+M_A)}{r\eta_A}, \frac{(\eta_A+M_A)(M_Y+\beta_Y)}{r\eta_A\beta_Y}, W_3\frac{(M_{fr}+\mu_{fr})}{\mu_{fr}}, W_3\frac{(M_f+\mu_{fr})(M_f+\mu_{rb})}{\mu_{fr}\mu_{rb}}\right)^T$$

It is easy to verify that $V(\mathbf{0}) = 0$, and $V(x) > 0$, for all $x > 0$. Moreover, we have

$$\dot{V}(x) =< W, A(x)x >= u_b(N_{Egg} + W_3 - W_5) - \frac{N_{Egg}}{K}u_A.$$

In particular, we have

$$\begin{aligned} N_{Egg} + W_3 - W_5 &= N_{Egg} + W_3\mu_{bf}\left(1 - \frac{(M_f+\mu_{fr})(M_f+\mu_{rb})(M_f+\mu_{bf})}{\mu_{fr}\mu_{rb}\mu_{bf}}\right) \\ &= N_{Egg} - W_3\mu_{bf}\left(\frac{(M_f+\mu_{fr})(M_f+\mu_{rb})(M_f+\mu_{bf})}{\mu_{fr}\mu_{rb}\mu_{bf}} - 1\right) \\ &= \frac{(\eta_A+M_A)(M_Y+\beta_Y)}{N_{Egg}\mu_{bf}\mu_{fr}\mu_{rb}r\eta_A\beta_Y}\left(1 - \frac{1}{R_0}\right). \end{aligned}$$

Thus, we deduce that $N_{Egg} + W_3 - W_5 \leq 0$ when $R_0 \leq 1$. Thus, we deduce that $\dot{V}(x) < 0$ when $R_0 \leq 1$. Moreover the maximal invariant set contained in $\dot{V} = 0$ is $\mathbf{0}_5$. Thus, from LaSalle-Lyapunov theory, we deduce that $\mathbf{0}_5$ is GAS in $\mathbb{R}^5_+$ for system $\frac{dx}{dt} = f(x)$. Finally, using the fact 0 is GAS in $\mathbb{R}_+$ for system $\frac{dy}{dt} = g(0_5, y)$, using theorem 3 in [52] (see also [31]), we deduce that $TE = \mathbf{0}_6$ is GAS in $\mathbb{R}^6_+$.

Finally, Model (1) being an extension of the model studied in [23], the global asymptotic stability of equilibrium E can be proved using the same approach than in [23]. The computations being long and tedious, we don't develop them.

Remark 4. *As an alternative to the proof of theorem 1, we could show that system (1) is monotonous and cooperative and apply the results developed by Anguelov et al. [1].*